Available online at www.sciencedirect.com

ScienceDirect

Procedia Manufacturing 15 (2018) 6–13

Procedia MANUFACTURING

www.elsevier.com/locate/procedia

17th International Conference on Metal Forming, Metal Forming 2018, 16-19 September 2018, Toyohashi, Japan

Experimental and modelling techniques for hot stamping applications

Zhutao Shao[a], Jianguo Lin[a,*], Mani Ganapathy[a], Trevor Dean[b]

[a]*Department of Mechanical Engineering, Imperial College London, London SW7 2AZ, UK*
[b]*School of Mechanical Engineering, University of Birmingham, Birmingham B15 2TT, UK*

Abstract

Hot stamping techniques have been developed for the production of complex-shaped components since the 1970s, increasingly used for the automotive industry. The application of these techniques includes hot stamping of boron steel for critical automobile safety components, and solution heat treatment, forming and cold die quenching (HFQ®) for forming complex-shaped high strength aluminium panels of automobile bodies and chassis structures. The developed forming techniques need dedicated experimental testing methods to be improved for characterising the thermomechanical behaviour of materials at the hot stamping conditions, and advanced materials modelling techniques to be developed for hot stamping applications. In this paper, requirements for thermomechanical tests and difficulties for hot stamping applications are introduced and analysed. The viscoplastic modelling techniques have been developed for hot stamping applications. Improved experimental methods have been proposed and used in order to obtain accurate thermomechanical uniaxial tensile test data and determine forming limits of metallic materials under hot stamping conditions.

Peer-review under responsibility of the scientific committee of the 17th International Conference on Metal Forming.

Keywords: Sheet metal forming; Hot stamping; Thermomechanical properties; Formability; Materials modelling

1. Introduction

The automotive industry is facing a huge global challenge to reduce fuel consumption and minimise

* Corresponding author. Tel.: +44-207-594-7082; fax: +44-207-594-7017.
E-mail address: jianguo.lin@imperial.ac.uk

2351-9789
Peer-review under responsibility of the scientific committee of the 17th International Conference on Metal Forming.
10.1016/j.promfg.2018.07.164

environmental pollution from vehicle emissions. Ultra high strength steels and lightweight materials are widely used to manufacture automobile structural components in order to reduce vehicle weight, improve safety and crashworthiness [1]. For example, aluminium alloy is a suitable lightweight material because it has reasonable strength and it provides a weight saving of up to 40% over steel in most applications [2]. At room temperature, ultra high strength steel is difficult to form and aluminium alloy has low formability, which leads to high springback and poor surface quality of formed components. To overcome this problem, hot forming technologies have been developed and experienced tremendous development in automotive applications. They are hot stamping and cold die quenching of quenchable steel sheets [3] and solution heat treatment, forming and cold die quenching (HFQ®) of lightweight alloys.

Various analytical and numerical models have been developed for characterising material mechanical behaviour and predicting formability of metallic materials at room temperature. These have been reviewed by Banabic et al. [4] and Stoughton et al. [5]. Since microstructural evolution in an alloy has a significant and different effect on materials properties at elevated temperature, a developed modelling technique by applying accurate constitutive data relevant to processing conditions is needed in order to optimise the hot forming processes and characterise thermomechanical response for different alloys.

However, existing standards are applicable only for thermomechanical testing under isothermal or near isothermal conditions with a small temperature deviation within the gauge region of a specimen [6]. In order to characterise alloy properties subjected to hot stamping processes, rapid heating and cooling on a specimen must be the integral process of a uniaxial tensile test. Performing uniaxial tensile tests in a Gleeble [7] can be considered as an alternative method, but the non-uniform temperature distribution within the gauge length of a test-piece results in inhomogeneous deformation due to the unavoidable heat loss at the two ends of the specimen. Therefore, the accuracy of strain measurement in a Gleeble under hot stamping conditions needs to be improved.

The development of most hot forming processes involves improvement of sheet metal formability which is usually evaluated by a forming limit diagram (FLD) determined at various deformation temperature and strain rate conditions [4]. Conventional out-of-plane and in-plane formability test methods are usually applicable for cold forming conditions and few formability tests have been conducted for sheet pressing processes at elevated temperature. It is very difficult to obtain forming limits of alloys under hot stamping conditions since special tooling and test procedures are usually needed and cooling occurs prior to deformation, which causes stable heating, cooling and deformation control is not easy to obtain. Therefore, formability test for hot stamping and HFQ® applications needs to be developed.

The aim of this research is to develop and verify unified multi-axial constitutive material models to be used for hot stamping applications by adopting accurate and validated thermomechanical and formability tests under hot stamping and HFQ® conditions.

Nomenclature

$\dot{\varepsilon}_e$	effective strain rate	k	initial yield point
σ_e	von-Mises stress	R	isotropic hardening
ω	damage	S_{ij}	deviatoric stress
$\dot{\varepsilon}_{ij}^P$	plastic strain rate	$\overline{\rho}$	normalized dislocation density
D_{ijkl}	elastic matrix of material	$\dot{\omega}$	damage evolution
R_g	universal gas constant	T	absolute temperature
Ω_0	pre-exponential factor of Ω	Q_Ω	activation energy of Ω
$A, n_2, \mu_1, \mu_{11}, \mu_{12}, \mu_2, \phi, \phi_{11}, \phi_{12}, \gamma, \Delta^*, \Delta_{11}^*, \Delta_{12}^*, \Delta_{21}^*, \Delta_{22}^*$			material constants

2. Unified viscoplastic damage constitutive equations

Lin et al. [8] proposed a dislocation-based viscoplastic damage model for analysis of forming processes at elevated temperatures. For hot stamping applications, a continuum damage mechanics (CDM)-based materials model was developed to describe the thermomechanical response of an alloy and to predict the formability of the metal. In this model, a set of unified viscoplastic damage constitutive equations was formulated [8] to capture the features of stress-strain curves and forming limit curves of sheet metals under hot stamping conditions.

$$\dot{\varepsilon}_e = \left\{ \left[\left| \sigma_e / (1-\omega) \right| - R - k \right] / K \right\}^{n_1}, \tag{1}$$

$$\dot{\varepsilon}_{ij}^{P} = 3 S_{ij} \dot{\varepsilon}_e / (2\sigma_e), \tag{2}$$

$$R = B \bar{\rho}^{0.5}, \tag{3}$$

$$\dot{\bar{\rho}} = A(1-\bar{\rho}) \left| \dot{\varepsilon}_e \right| - C \bar{\rho}^{n_2}, \tag{4}$$

$$\sigma_{ij} = (1-\omega) D_{ijkl} \left(\varepsilon_{ij} - \varepsilon_{ij}^{P} \right), \tag{5}$$

$$\dot{\omega} = \left[\Delta^* / (\mu_1 - 0.5\mu_2)^{\phi} \right] \left[(\mu_1 \varepsilon_1 + \mu_2 \varepsilon_2) / (\gamma + \varepsilon_P) \right]^{\phi} \left[\eta_1 (\dot{\varepsilon}_e)^{\eta_2} / (1-\omega)^{\eta_3} \right], \tag{6}$$

where the temperature-dependent parameters in Eqs. (1)-(6) are defined as the form of Arrhenius equation for HFQ® applications:

$$\Omega = \Omega_0 \exp\left[Q_\Omega / (R_g T) \right], \tag{7}$$

where Ω stands for temperature dependent parameters, including K, k, n_1, B, C, η_1, η_2, η_3 and E. Q_Ω stands for corresponding activation energy items Q_K, Q_k, Q_{n_1}, Q_B, Q_C, Q_{η_1}, Q_{η_2}, Q_{η_3} and Q_E. Parameters of μ_1, ϕ and Δ^* are expressed in Eqs. (8)-(10).

$$\mu_1 = \mu_{11} \exp(-\mu_{12}/T), \tag{8}$$

$$\phi = \phi_{11} \exp(-\phi_{12}/T), \tag{9}$$

$$\Delta^* = \Delta_{11}^* \exp(\Delta_{12}^*/T) + \Delta_{21}^* \exp(\Delta_{22}^* \dot{\varepsilon}_e). \tag{10}$$

Eq. (1) is the flow rule, in which effective strain rate is formulated by using the traditional power law with damage ω taken into account. Eq. (3) is a function of the normalised dislocation density $\bar{\rho}$. Eq. (4) represents dynamic and static recovery and the accumulation of dislocations due to plastic flow. The flow stress equation was modified to include the effect of damage in Eq. (5). The first two terms in Eq. (6) are proposed to describe the effects of major strain and minor strain on the damage evolution in the material. Temperature and strain rate dependent parameters are introduced in Eq. (6) to control the predicted FLD of the material. Parameters can be presented in terms of functions of martensite volume fraction and combined with austenite formation to predict the thermomechanical response of born steel [9, 10]. All material constants need to be determined by experimental data of tensile tests and formability tests obtained under hot stamping or HFQ® conditions.

3. Thermomechanical tensile tests under hot stamping conditions

Using digital image correlation (DIC) is a good non-contact method for strain measurement of deformation history and it has been widely used and accepted in the field of experimental mechanics. One high-speed camera can be employed for capturing the images and measuring in-plane deformation. A set of purpose-built grips (as shown in Fig. 1 (a)) were designed to clamp specimens and make the specimen surface parallel to the high-speed camera in order to use the DIC system for strain measurement. In a Gleeble, the material, size and features of grips have effects on the temperature distribution of a specimen clamped, given that cooling channel in the jaws takes away heat from the two grips during a resistance heating process. In general, copper grips have a higher thermal conductivity than stainless steel ones but with a lower stiffness. In order to reduce heat loss, the grips can be designed to be thermally insulated with the cooled jaw [11], as shown in Fig. 1 (b). Both types of grips enable uniaxial tensile tests to be performed accurately by using the DIC strain measurement system under complex heating and cooling conditions.

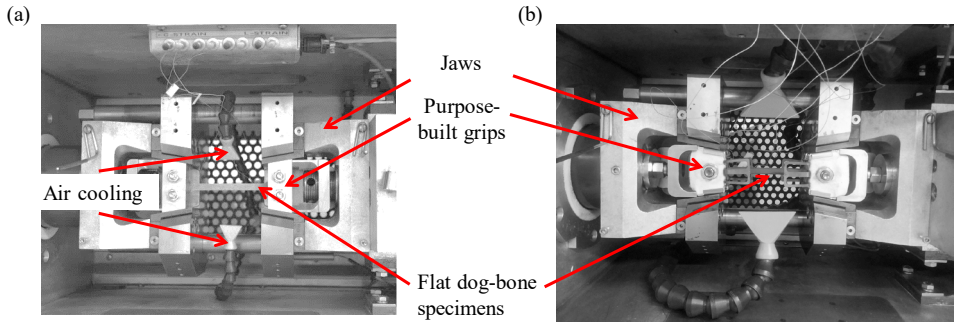

Fig. 1. Two purpose-built grips (a) made of stainless steel; (b) thermal insulated with jaws, mounted in Gleeble chamber for thermomechanical testing by using DIC system.

As an example, thermomechanical tensile tests of AA6082 was conducted at the temperatures of 400-500 °C and strain rates of 0.1-4 /s after 1 min soaking at 535 °C. The stress-strain curves were characterised under various deformation conditions and material constants in Eqs. (1)-(5) related to the characterisation of the thermomechanical response of the material were determined, as shown in Table 1. In Fig.2, good agreement has been obtained for AA6082 at all test conditions. This indicates that the thermal-activated mechanisms described by Arrhenius' law are applicable for AA6082 at elevated forming temperatures.

Table 1. Material constants related to thermomechanical response in Eqs. (1)-(6) for AA6082 deformed under HFQ® conditions.

K_0 (MPa)	k_0 (MPa)	n_{0_1}	B_0 (MPa)	C_0	η_{1_0}	η_{2_0}	η_{3_0}
0.36	0.59	0.10	4.83	7.31	2.46	0.84	0.24
Q_K (J/mol)	Q_k (J/mol)	Q_{n_1} (J/mol)	Q_B (J/mol)	Q_C (J/mol)	Q_{η_1} (J/mol)	Q_{η_2} (J/mol)	Q_{η_3} (J/mol)
25409.5	21693.0	17637.1	15698.9	2112.6	16273.2	837.8	22107.9
Q_E (J/mol)	R (J/molK)	E_0 (MPa)	A	n_2			
27987.4	8.31	249.7	0.19	1.83			

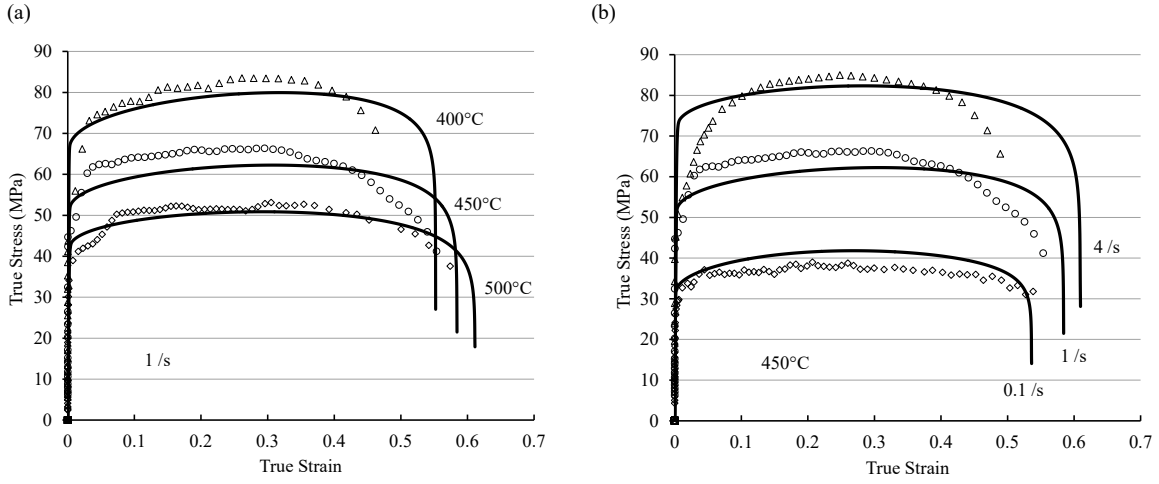

Fig. 2. Comparison of experimental (symbols) and numerical integrated (solid curves) true stress-true strain curves of AA6082 at various (a) temperatures and (b) strain rates.

4. Formability tests under hot stamping conditions

A biaxial testing system based on a Gleeble has been developed and used for formability tests under complex hot stamping conditions [12]. This biaxial apparatus can convert a uniaxial force exerted by the Gleeble into a biaxial state and it can be considered as a linkage mechanism with four independent servo-hydraulic actuators, which enables to obtain a symmetric strain distribution within central region of a cruciform specimen since the biaxial loaded region on a specimen remains still to avoid bending moments [13]. The displacements D_1, D_2 are equal and collinear to the displacement D_1^* and D_2^*, respectively. The testing system used for formability tests has a relatively simple configuration (as shown in Fig. 3 (c)) and it is employable within limited space with a high loading capacity.

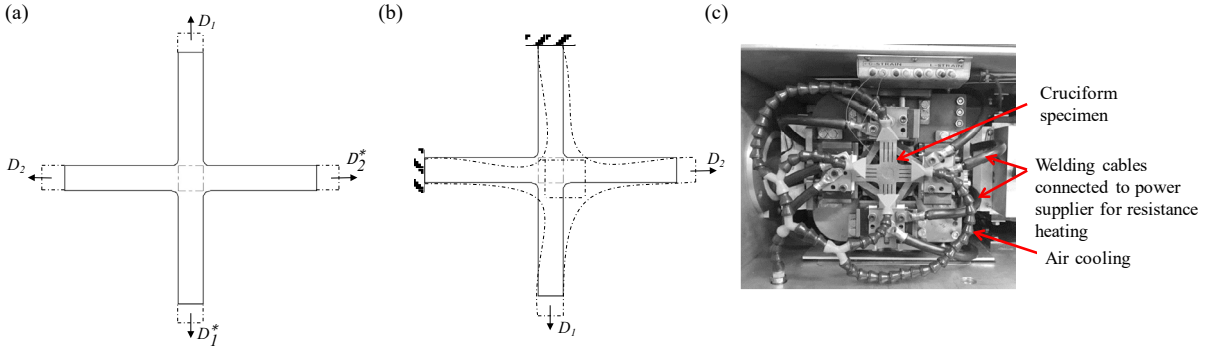

Fig. 3. Schematics of cruciform specimen deformed with (a) four actuators and (b) two actuators biaxial machines, and (c) picture of experimental set-up of biaxial formability tests.

For formability tests under HFQ® conditions, the material of AA6082 was deformed at a designated temperature in the range of 370-510 °C and at a deformation strain rate of 0.01-1 /s after 1 minute soaking at 535 °C. Linear strain path condition contains uniaxial, plane strain and biaxial testing, in order to determine an FLD of the material. The biaxial testing system is capable of performing strain measurement by using DIC. Friction effects, which could cause errors on the measurement of FLDs of alloys, were avoided, and a constant effective strain rate and approximate isothermal condition in a specimen were realised during testing. The calibrated material constants for AA6082 related to formability prediction in Eqs. (6)-(10) under HFQ® conditions are shown in Table 2.

Table 2. Material constants related to formability prediction in Eqs. (6)-(10) for AA6082 deformed under HFQ® conditions.

μ_{11}	μ_{12}	μ_2	ϕ_{11}	ϕ_{12}
0.85	451.9	0.15	19.09	874.6
Δ_{11}^*	Δ_{12}^*	Δ_{21}^*	Δ_{22}^*	γ
79.8	26.1	-81.1	3.52E-3	3.5E-3

Forming limit data for different strain paths were determined and hence the FLDs for HFQ® conditions were obtained through curve fitting and are shown in Fig. 4. It is found that when the strain rate increases from the designated strain rate of 0.01 /s to 1 /s, the forming limit of AA6082 increases. The forming limit has a larger increase from 0.1 /s to 1 /s than that from 0.01 /s to 1 /s and a monotonic increase is observed in forming limit from the temperature of 370 °C to 510 °C. This means that good formability for AA6082 can be obtained at a relatively high temperature under HFQ® conditions. Forming limit curves on the left-hand side of the FLD are close to each other, which indicates the higher sensitivity of temperature dependence for the material under tension-tension biaxial strain paths compared to that under tension-compression strain paths. In summary, higher forming speeds and higher temperatures within the designated ranges are beneficial for enhancing the forming limits of AA6082 under HFQ® conditions.

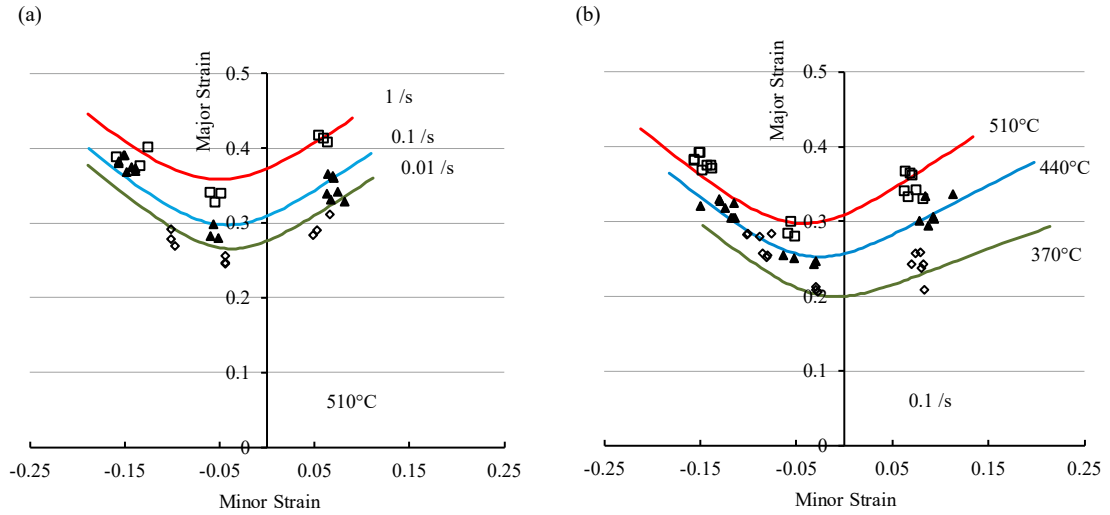

Fig. 4. FLDs of A66082 determined by experimental tests (symbols) and computed by materials model (solid lines) under various (a) strain rates and (b) deformation temperatures.

5. Discussions

5.1. Effect of strain rate on flow stress response and formability

Higher flow stress with increasing strain rate can be observed, which reveals the strain rate sensitivity of viscous stress for the testing material of AA6082. High strain rate sensitivity is attributed to an increased rate of thermally activated processes, such as grain boundary sliding and dislocation climb [14]. The increase of flow stress with increasing strain mainly results from work hardening, which is caused by dislocation accumulation and interaction [15]. Due to dynamic and static recovery processes, close to the failure stage, the increasing trend is reduced through the annihilation of pairs of dislocations and relaxation of internal stresses [16]. Static recovery is related to deformation time. Dislocation density is more reduced at a lower strain rate so that working hardening is lower than that at a higher strain rate.

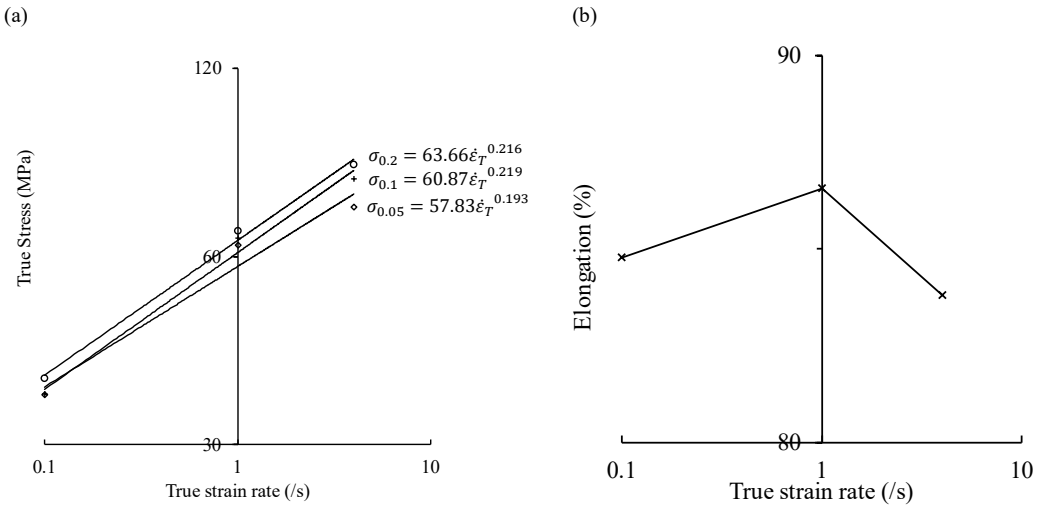

Fig. 5. (a) Flow stress at different strain levels (0.05, 0.1 and 0.2) for different designated strain rates at the designated temperature of 450°C; (b) elongation at the deformation temperature of 450°C at different strain rates.

Fig. 5 (a) is a summary of stress values at three true strain levels (0.05, 0.1 and 0.2) for various designated strain rates at the deformation temperature of 450 °C. Power fits, which suggest the power law viscoplastic response of both materials, are shown in the figure by plotting logarithmic stress verse logarithmic strain rate. It can be seen that the increase of stress with increasing strain rate exhibits the strain rate hardening characteristic and the strain rate exponent corresponds to the power exponent in the equations. The strain rate hardening exponent is a critical factor influencing the uniformity of deformation during forming processes. Strain hardening and strain rate hardening are beneficial to the uniformity of material flow and internal stress transfer in the material, which can reduce the tendency to localised necking and thus higher formability, as shown in Fig. 4 (a). Fig. 5 (b) shows the values of elongation at the testing temperature of 450 °C at different strain rates. It is not a monotonic increasing trend and the materials have the largest elongation at the designated strain rate of 1 /s, but material at all conditions has over 80% of elongation, which indicates good formability in this range of strain rate. The difference between the values of elongation under this test condition for the material of AA6082 is 3.2% for the material.

5.2. Effect of temperature on flow stress response and formability

AA6082 has strong temperature sensitivity according to the test results and this is typical of most metals since many deformation associated processes are thermally activated. Fig. 6 (a) summarises the flow stress values at various strain levels for deformation temperatures of 400 °C, 450 °C and 500 °C by plotting logarithmic stress against inverse temperature. The stress level and strain hardening decrease with increasing temperature for the material. The near rectilinear fit indicates the standard Arrhenius activation energy equation enables temperature dependence of flow stress to be described even though a small deviation from linearity for materials is observed at the low strain level of 0.05.

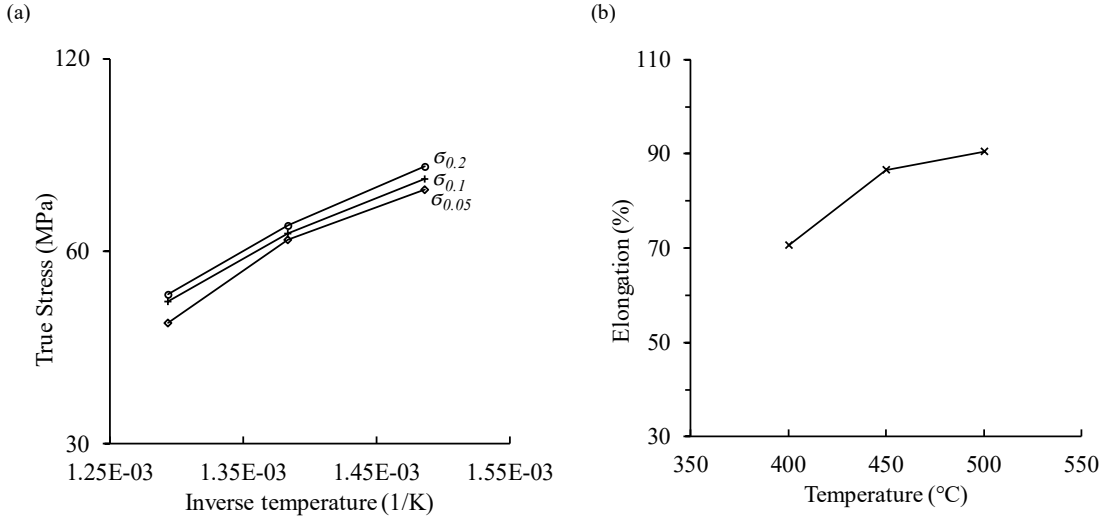

Fig. 6. (a) Flow stress at different strain levels (0.05, 0.1 and 0.2) for different deformation temperatures (designated strain rate is 1 /s); (b) elongation at designated strain rate of 1 /s for different temperatures.

At elevated temperature, increased thermal vibration of the microstructural lattice enhances dislocation mobility, thus lower flow stress is required to overcome activation barriers [14]. Sliding and rotation of grain boundary and microstructural recovery are more activated with the increasing temperature, which results in higher ductility. Fig. 6 (b) shows higher ductility at a higher temperature. Over a 100 °C temperature range, the difference between values of elongation for the material is 22%. The material has relatively high temperature sensitivity, at the temperature of 500 °C, and it performs good formability due to the largest elongation observed, which benefits the formability, as shown in Fig. 4 (b).

6. Conclusions

One type of physically-based viscoplastic-damage constitutive model has been developed to describe the deformation behaviour of alloys and to predict formability of alloys under hot stamping conditions. It takes the mechanisms of dislocation-driven evolution processes, such as work hardening, dynamic and static recovery and damage, into account. The effects of temperature and strain rate on the thermomechanical response and formability of aluminium alloys are modelled. The data generated from improved uniaxial and biaxial formability tests were used to calibrate and validate all the equations. The determined models give an accurate prediction of forming limits of AA6082 so that material failure can be modelled under HFQ® conditions. The accuracy of determined FLD was analysed by consideration of temperature and strain rate effects obtained from the thermomechanical uniaxial tensile test. It was found that the material of AA6082 exhibited high formability at high temperature and high strain rate. The experimental and modelling techniques have been established and can be used to evaluate thermomechanical properties and formability of metallic materials under hot stamping conditions.

Acknowledgement

The authors gratefully acknowledge the financial support from EPSRC (Grant Ref: EP/I038616/1) for TARF-LCV: Towards Affordable, Closed-Loop Recyclable Future Low Carbon Vehicle Structures. HFQ® is a registered trademark of Impression Technologies Limited. Impression Technologies Limited is the sole licensee for the commercialisation of the HFQ® technology from Imperial College London.

References

[1] H. Karbasian, A.E. Tekkaya, A review on hot stamping, Journal of Materials Processing Technology, 210 (2010) 2103–2118.
[2] K.R. Brown, M.S. Venie, R.A. Woods, The increasing use of aluminium in automotive applications, JOM, 47 (1995) 20–23.
[3] R. George, A. Bardelcik, M.J. Worswick, Hot forming of boron steels using heated and cooled tooling for tailored properties, Journal of Materials Processing Technology, 212 (2012) 2386–2399.
[4] D. Banabic, F. Barlat, O. Cazacu, T. Kuwabara, Advances in anisotropy and formability, International Journal of Material Forming, 3 (2010) 165–189.
[5] T.B. Stoughton, X. Zhu, Review of theoretical models of the strain-based FLD and their relevance to the stress-based FLD, International Journal of Plasticity, 20 (2004) 1463–1486.
[6] Tensile testing of metallic materials-Part 5: Method of test at elevated temperatures, In International Organization for Standardization, ISO, 6892-2 (2011).
[7] DSI, Gleeble system, In Dynamic Systems Inc.
[8] J. Lin, M. Mohamed, D. Balint, T.A. Dean, The development of continuum damage mechanics-based theories for predicting forming limit diagrams for hot stamping applications, International Journal of Damage Mechanics, 23 (2013) 684–701.
[9] N. Li, J.G. Lin, T.A. Dean, Development of unified viscoplastic-damage model for crashworthiness analysis of boron steel safety components with tailored microstructures, Applied Mechanics and Materials, 784 (2015) 427–434.
[10] N. Li, J. Lin, D.S. Balint, T.A. Dean, Modelling of austenite formation during heating in boron steel hot stamping processes, Journal of Materials Processing Technology, 237 (2016) 394–401.
[11] M. Ganapathy, N. Li, J. Lin, M. Abspoel, D. Bhattacharjee, A novel grip design for high-accuracy thermo-mechanical tensile testing of boron steel under hot stamping conditions, Experimental Mechanics, 58 (2017) 243–258.
[12] Z. Shao, N. Li, J. Lin, T.A. Dean, Development of a new biaxial testing system for generating forming limit diagrams for sheet metals under hot stamping conditions, Experimental Mechanics, 56 (2016) 1489–1500.
[13] A. Smits, D.V. Hemelrijck, T.P. Philippidis, A. Cardon, Design of a cruciform specimen for biaxial testing of fibre reinforced composite laminates, Composites Science and Technology, 66 (2006) 964–975.
[14] W.F. Hosford, R.M. Caddell, Metal forming: mechanics and metallurgy, fourth edition, Cambridge University Press, New York, (2011).
[15] J. Lemaitre, J.L. Chaboche, Mechanics of solid materials, Cambridge University Press, (1990).
[16] J. Lin, Y. Liu, D.C.J. Farrugia, M. Zhou, Development of dislocation-based unified material model for simulating microstructure evolution in multipass hot rolling, Philosophical Magazine, 85 (2005) 1967–1987.